

Color measurement: comparison of colorimeter vs. computer vision system

Sandro M. Goñi^{1,2} · Viviana O. Salvadori^{1,2}

Received: 23 February 2016 / Accepted: 3 October 2016 / Published online: 17 October 2016
 © Springer Science+Business Media New York 2016

Abstract The aim of this work was to compare two food color measurement techniques, the traditional tristimulus colorimeter and an image analysis system. In this sense a computer vision system was developed, consisting of a digital camera, a controlled illumination environment, and a software package to process the images. The conversion between color spaces was performed employing empirical mathematical models; a standard color chart was used for its calibration. The color of 40 samples of raw and processed foods was measured in the *CIELAB* color space with the computer vision system and a colorimeter. The equivalence between both techniques, for individual L^* , a^* and b^* values, was determined using appropriate hypothesis tests. For most samples both systems provide equivalent results, although the total color difference ΔE was high enough to be noticeable. The average ΔE was 5.88 ± 3.32 , with an average absolute $\Delta L^* = 2.79 \pm 2.42$, $\Delta a^* = 3.02 \pm 2.94$; $\Delta b^* = 2.84 \pm 2.53$. In addition, the color measured by the image analyses technique seemed to be more similar to the real ones.

Keywords Food color · Computer vision · Digital images · Image processing · Color calibration

Introduction

Food color, in both raw and processed products, is one of the main quality characteristics, since it is the first aspect that is perceived by consumers and it can determine the acceptance of a product [1, 2]. In the food science and technology field color is traditionally represented using the CIE 1976 $L^*a^*b^*$ or *CIELAB* color space [3]. Commonly the measurements are performed using tristimulus colorimeters [1, 2]. Although colorimeters are easy to use and calibrate, the measurement area is very small (only a few cm^2), besides it must be in contact with the sample, limiting their use in industrial applications and on-line monitoring. Furthermore, its acquisition cost is relatively high, as well as its repair and replacement parts [2].

The use of digital images in food analysis has considerably increased in the last years, showing numerous and varied applications [4, 5]. In particular, many studies focused in determining food color in the *CIELAB* space make use of digital imaging. One key aspect of using digital images involves the information processing, since the cameras obtain *RGB* (red, green and blue) values, which need to be transformed to *CIELAB* color space. Recently, Wu and Sun [2] published a complete review on different aspects of food color measurement using digital images. Literature shows two general approaches, the first being direct theoretical conversion [6–17], and the second being empirical conversion models [18–25]; some authors employed and compared both approaches [26, 27].

In order to measure color from digital images in a standardized manner, a computer vision system (*CVS*) is required. This system consists of a digital camera, an image acquisition chamber, a controlled illumination system and software to process the obtained information. A system of such characteristics overcomes the colorimeter's

✉ Sandro M. Goñi
 smgoni@quimica.unlp.edu.ar

¹ Centro de Investigación y Desarrollo en Criotecnología de Alimentos (CIDCA) CCT-CONICET, La Plata, Univ. Nacional de La Plata, 47 y 116, B1900AJJ La Plata, Argentina

² Facultad de Ingeniería, Univ. Nacional de La Plata, 1 y 47, B1900TAG La Plata, Argentina

limitations; in this sense very small as well as very large samples can be processed [28, 29], the CVS does not require direct contact with the sample, and it can be used remotely which is very advantageous for on-line monitoring in industrial processing. In regards to digital cameras, the market offers a large variety of brands, models and price, being the latter considerably lower than that of colorimeters [2, 21, 27]. As for the software, we have found that, in spite of the great number of reported studies and the advantages of this technique, simple computational tools for the processing of the CVS information are scarce (see for instance [16, 20]). This fact restricts its spreading since the software development is a limiting constraint for many potential users.

A few studies compared the results obtained from digital images and colorimeters for particular foods. The work of Leon et al. [26] was focused on the conversion between color spaces and the calibration process; the authors validated the developed system with the color of a potato chip measured by a colorimeter, using the Hunter Lab color space. Yagiz et al. [30] measured irradiated salmon samples using *CIELAB* color space; they found deep differences between the colors predicted by both approaches. It is worth to note that the color of the analyzed samples has a narrow gamut, close to light-brown with the colorimeter and to salmon-pink with the computer vision system. Girolami et al. [31] measured the color of different kind of meat samples, also using *CIELAB* color space, and found substantial differences between both devices. The color of the analyzed samples also has low variability, close to red or pale-brown.

Hence, the objective of this work was to assess the equivalence between color values measured from a computer vision system and a traditional colorimeter, employing food samples of a wide gamut of colors and nature. For this aim, a CVS was constructed, which can be tested or calibrated using the classic X-Rite ColorChecker rendition chart, not requiring a colorimeter. For the image processing a software package, previously developed and free available, was used.

Materials and methods

Computer vision system (CVS) development

Image acquisition system

The image acquisition system consisted of an image acquisition chamber, an illumination system and a digital camera (Fig. 1).

The image acquisition chamber was made of wood and painted in black in order to diminish internal light reflections. It was composed of four laterals walls (three fixed and one mobile) and a floor with adjustable height. The illumination system, consisting of four fluorescent tube holders, 60 cm

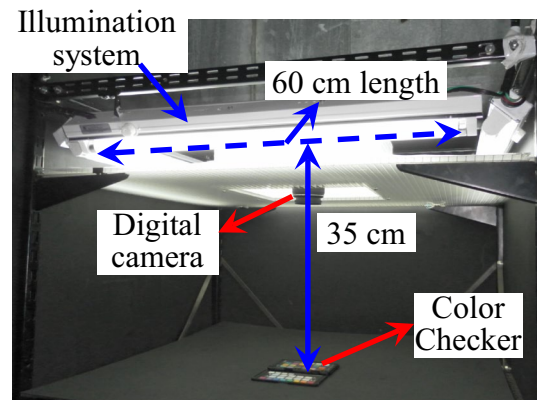


Fig. 1 Image acquisition chamber used for the CVS

length (22 W Verbatim fluorescent tubes were used), was placed on the top of the chamber. A removable diffuser was located under the illumination system, to avoid the direct incidence of the light over the samples. Finally, a generic moving mount was used to hold the digital camera above the system. The distance between each pair of fluorescent tubes was of 70 cm, and the chamber floor height was regulated to provide a distance of 35 cm between the digital camera and the sample.

To analyze the influence of the digital camera characteristics on the goodness of the CVS performance, two cameras were used for image acquisition in this work; the details of their characteristics and settings are summarized in Table 1.

Image processing

The image processing was performed by a software package developed in the form of simple and user friendly

Table 1 Basic characteristics and configuration of the employed digital cameras

	Digital camera	
	NIKON D3100	Samsung ST60
Mode	Manual	Program, Macro on
Maximum image size	4608×3072	4000×3000
Image size used in the experiments	2304×1536	2048×1536
ISO sensitivity	100	100
Flash	Off	Off
Diaphragm aperture	f/5.6	Automatic
Exposure time	1/8	Automatic
Focus	Automatic	Automatic
White balance	Daylight fluorescent	White fluorescent lighting
Zoom	Manual	Manual
Image format	jpeg	jpeg

graphics interfaces, using MATLAB® (The Mathworks Inc., Natick, Mass., USA). This software can be free download through the UNLP-SeDICI repository (<http://hdl.handle.net/10915/45660>); a detailed User Guide and also a brief guide for its installation are available.

Mainly, the software allows calibrating the *CVS*, and performing the *RGB* to *L*a*b** color conversion and also the inverse conversion, from *L*a*b** to *RGB*. Different color space conversion models were implemented.

Direct conversion model

This is the simplest conversion model, since it does not require calibration; it is good for ideal systems, i.e. with a correctly set camera and standard illumination conditions [32]. The steps involved are as follows:

1. Given a color image of *n* bits by color layer, scale it to the [0.1] interval [Eq. (1)], where *RGB_O* and *RGB_S* contain the Red, Green and Blue components of each pixel of the original and scaled images, respectively. In this work images of eight bits were used.

$$RGB_S = \frac{RGB_O}{2^n} \tag{1}$$

2. The scaled image is converted to *XYZ* tristimulus values using the *g* function [33]:

$$XYZ = \begin{pmatrix} 0.4124 & 0.3575 & 0.1804 \\ 0.2126 & 0.7151 & 0.0721 \\ 0.0193 & 0.1191 & 0.9504 \end{pmatrix} g(RGB_S) \tag{2}$$

$$g(x) = 100 \begin{cases} \left(\frac{x+0.055}{1.055}\right)^{2.4}, & x > 0.04045 \\ \frac{x}{12.92}, & x \leq 0.04045 \end{cases} \tag{3}$$

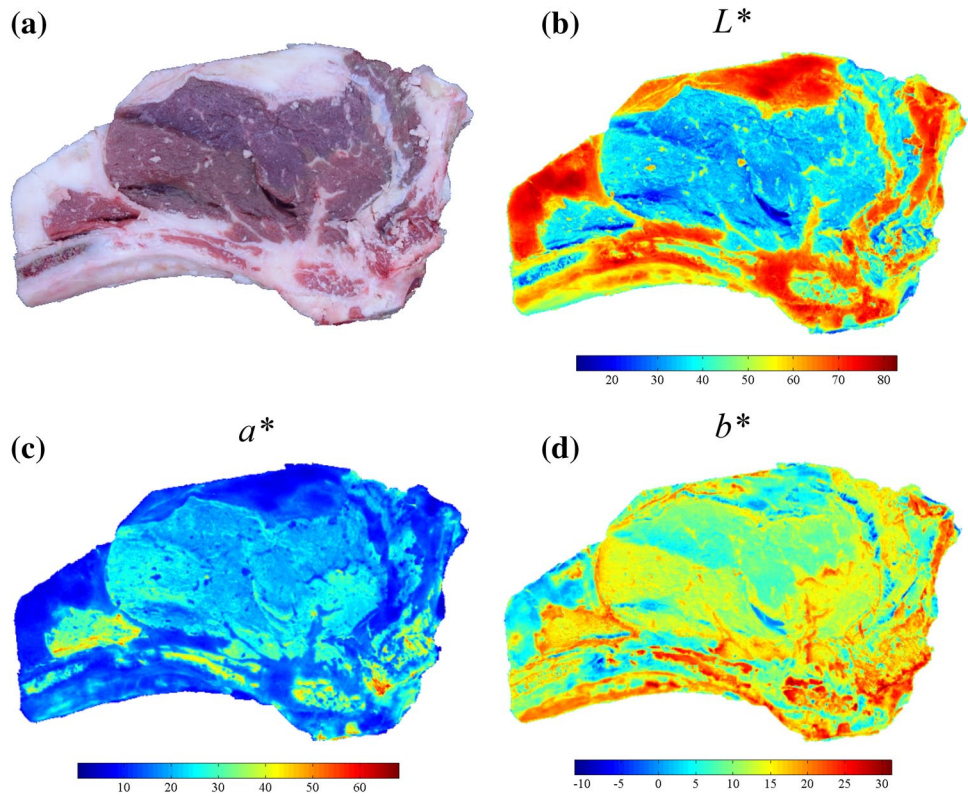
3. The *XYZ* tristimulus values are converted to *L*a*b** values using the *h* function [3, 35]:

$$\begin{cases} L^* = 116h\left(\frac{Y}{Y_R}\right) - 16 \\ a^* = 500\left(h\left(\frac{X}{X_R}\right) - h\left(\frac{Y}{Y_R}\right)\right) \\ b^* = 200\left(h\left(\frac{Y}{Y_R}\right) - h\left(\frac{Z}{Z_R}\right)\right) \end{cases} \tag{4}$$

Table 2 Fitting performance of the empirical conversion models, using different digital cameras

Conversion model	Average		ΔE	
	ΔL*	Δa*		
Nikon D3100, average error of ten calibration procedures	Linear, Eq. (7)	1.841 ± 0.082	3.720 ± 0.211	5.728 ± 0.222
	Quadratic, Eq. (8)	0.931 ± 0.032	2.715 ± 0.008	4.516 ± 0.178
	Quadratic plus interactions, Eq. (9)	0.621 ± 0.035	1.478 ± 0.043	2.085 ± 0.226
Samsung ST60, average error of five calibration procedures	Linear, Eq. (7)	2.286 ± 0.028	4.253 ± 0.227	6.613 ± 0.829
	Quadratic, Eq. (8)	1.335 ± 0.154	2.215 ± 0.238	4.415 ± 0.481
	Quadratic plus interactions, Eq. (9)	0.824 ± 0.076	1.611 ± 0.212	2.506 ± 0.597

Fig. 2 Color results obtained for a beef steak sample. **a** Image of the sample. **b** Predicted L^* values; **c** predicted a^* values; **d** predicted b^* values. (Color figure online)



$$h(x) = \begin{cases} x^3, & x > \left(\frac{6}{29}\right)^3 \\ \frac{1}{3} \left(\frac{29}{6}\right)^2 x + \frac{4}{29}, & x \leq \left(\frac{6}{29}\right)^3 \end{cases} \quad (5)$$

The X_R, Y_R, Z_R are the reference tristimulus values of the D_{65} illuminant, which have white trichromatic coefficients $x_R=0.3127, y_R=0.3290$ (and $z_R=1-x_R-y_R$), and a luminance value $Y_R=100$. The values of X_R y Z_R can be then obtained from Eq. (6):

$$\begin{cases} X_R = \frac{x_R}{y_R} Y_R \\ Z_R = \frac{z_R}{y_R} Y_R \end{cases} \quad (6)$$

Empirical conversion models

In contrast to the direct models, the empirical models can be applied when the illumination conditions are not the standard ones, what is a clear advantage. However, they must be fitted through a calibration procedure using samples with known color values.

The used empirical conversion models were polynomial expressions, which relate the $L^*a^*b^*$ values with linear and quadratic relations, as well as interactions between the RGB color values, Eqs. (7–9) respectively:

$$L^*, a^*, b^* = \alpha_1 R + \alpha_2 G + \alpha_3 B + \alpha_4 \quad (7)$$

$$L^*, a^*, b^* = \alpha_1 R + \alpha_2 G + \alpha_3 B + \alpha_4 R^2 + \alpha_5 G^2 + \alpha_6 B^2 + \alpha_7 \quad (8)$$

$$L^*, a^*, b^* = \alpha_1 R + \alpha_2 G + \alpha_3 B + \alpha_4 R^2 + \alpha_5 G^2 + \alpha_6 B^2 + \alpha_7 RG + \alpha_8 RB + \alpha_9 GB + \alpha_{10} RGB + \alpha_{11} \quad (9)$$

For the calibration, the X-Rite ColorChecker rendition chart (X-Rite Inc., Grand Rapids, Michigan, USA), which is a standard color reference used in several studies [21, 27, 31, 34], was employed. The chart is composed of 24 patches with different colors, for which the $L^*a^*b^*$ values under different illuminants are available [35]; in this work the D_{65} illuminant was used. The color chart, placed in the chamber floor, is photographed and its digital image processed. The average RGB values for each one of the 24 patches are calculated, and the reference $L^*a^*b^*$ values are known. Then the unknown parameters of the conversion models are obtained by regression. Note that since the models have a linear dependence on their parameters, their fitting is simple.

In order to estimate the error of the calibration procedure, the average absolute residuals [Eq. (10), c^* refers to L^*, a^*

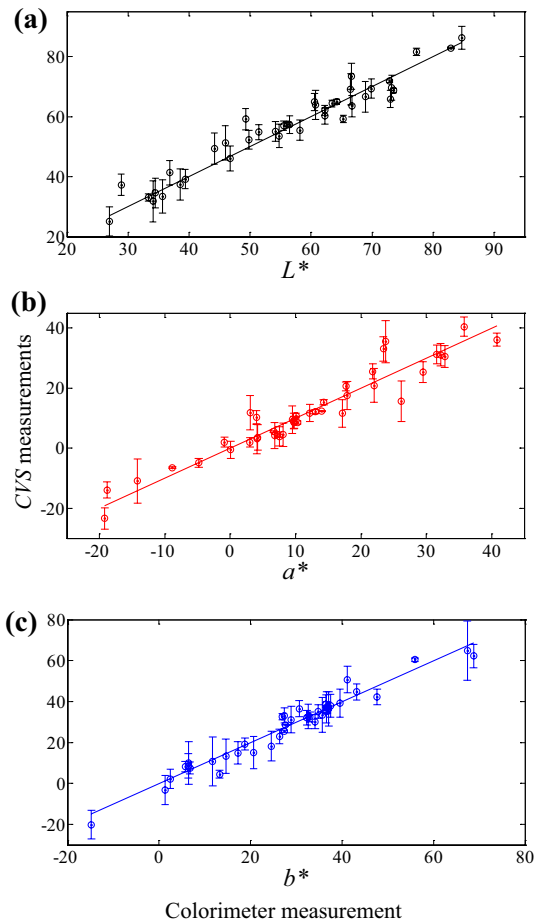


Fig. 3 Correlation between $L^*a^*b^*$ color values of the 40 food samples measured with the CVS and the colorimeter. Continuous error bars represent standard deviations of the CVS measurements. **a** L^* values. **b** a^* values. **c** b^* values. (Color figure online)

or b^*] and the total color difference ΔE [Eq. (11)] were calculated. The subscripts “Exp” and “Pred” refer to experimental and predicted values, respectively, being the experimental or reference values obtained from Pascale [35].

$$|\Delta c^*| = \frac{1}{m} \sum_{i=1}^m |c_{Exp,i}^* - c_{Pred,i}^*| \tag{10}$$

$$\Delta E = \frac{1}{m} \sum_{i=1}^m \sqrt{(L_{Exp,i}^* - L_{Pred,i}^*)^2 + (a_{Exp,i}^* - a_{Pred,i}^*)^2 + (b_{Exp,i}^* - b_{Pred,i}^*)^2} \tag{11}$$

Finally, it is worth to note that the user does not need a colorimeter to calibrate the CVS, since the reference color values of the ColorChecker can be obtained from bibliography, for different illuminants.

Color measurements

The surface color of 40 food samples were measured using two devices: the CVS developed in this work and a traditional

portable tristimulus colorimeter (Minolta CR-400), both using D_{65} illuminant. Different foods were used, both raw and processed: vegetables (carrot, cassava, lettuce, potato, pumpkin, purple cabbage, sweet potato, and tomato), fruits (apple, banana, lemon, nectarine, and orange), pieces of meats (beef, chicken breast, and sausage), bakery products (jam filled and colored glazed cookies, muffin, and sponge cake), etc.

Each sample, sometimes using a white tray to contain it, others only the sample, was placed inside the CVS chamber, in the middle of the chamber floor in order to obtain uniform illumination. Once placed, it was photographed, and then its surface color measured with the colorimeter. For statistical comparison purposes, three measurements were performed with the colorimeter for each sample, whereas a single digital image of each sample was employed (with thousands of pixels). The difference between the measurements obtained with both systems was assessed in a statistical way. First, a test of hypothesis on the equality of the variances was done; then a test of hypothesis on the equality of the means of samples with equal or different variance (depending on the result of the first test) was done [36]. All the tests were performed with a significance level $\alpha=0.05$. Also the difference between devices was determined using the average absolute residuals of $L^*a^*b^*$ values [Eq. (10)] and the total color difference [Eq. (11)].

Results and discussion

CVS calibration
















Table 2 presents the results of the CVS calibration employing the three implemented empirical models [Eqs. (7–9)]. A total of 15 calibration procedures was done, ten of them with the Nikon camera, the other five tested the Samsung camera. As regards the quality of these predictions, we have found that the results are satisfactory, independently from the digital camera.

As it was expected, the quadratic plus interactions model [Eq. (9)] provides lesser error, since it has a larger number of parameters. Leon et al. [26] found similar tendencies, although in their work they proposed a neural network with better performance.

The theoretical conversion model [Eqs. (1–5)] presented higher errors than the empirical ones (results not shown). This fact was influenced for the particular setup of the CVS used in the tests, however, a better illumination system and fine tuning of white balance of the digital cameras could improve predictions of the theoretical conversion model.

Respect to the digital cameras compared in the calibration procedure, it is worth to mention that there is a key difference between them. The Nikon camera can be

Fig. 4 Small *RGB* color images estimated from colorimeter and *CVS* measurements for different samples. The images of the samples are segmented from the background, and the central regions of the images were used to measure its *color*. The chicken sample, with highest ΔE , is shown. (Color figure online)

Sample	<i>CVS</i>		Colorimeter
Chicken (meat region)	L^* : 59.15 a^* : 11.87 b^* : 8.16		  L^* : 49.27 a^* : 3.04 b^* : 5.72
Lettuce	L^* : 52.35 a^* : -13.91 b^* : 30.18		  L^* : 44.16 a^* : -18.86 b^* : 34.15
Beef (meat region)	L^* : 34.60 a^* : 20.90 b^* : 10.87		  L^* : 34.51 a^* : 22.01 b^* : 11.74
Carrot	L^* : 55.06 a^* : 30.56 b^* : 42.28		  L^* : 54.16 a^* : 32.82 b^* : 47.69
Sausage (meat region)	L^* : 71.40 a^* : 11.34 b^* : 17.38		  L^* : 62.24 a^* : 17.14 b^* : 18.77

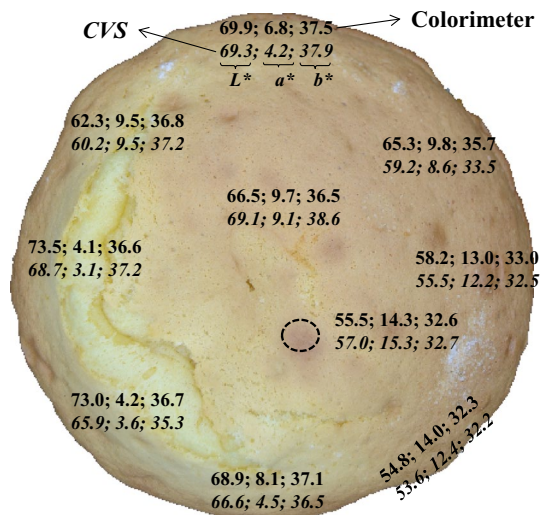


Fig. 5 $L^*a^*b^*$ color values in different regions of the sponge cake surface measured using the colorimeter and the *CVS*. (Color figure online)

used in full manual mode, so it can be calibrated once and then used to measure several samples through time. The other camera cannot be used in full manual mode, then each sample and the color chart must be acquired together (since the automatic tuning affects the measured color), and the calibration procedure must be executed in every measurement. For regular measurements this could

be laborious, but for occasional ones this aspect is not important. This feature demonstrates other strength of the developed methodology, that it provides accurate results although the camera setting changes from scene to scene. In this sense, the cited studies that employed empirical models and a calibration procedure [18–27], all of them developed using a particular digital camera, could potentially be used with any digital camera and different lighting conditions.

Color measurement

CVS performance

The superficial color of 40 foods, mentioned in “Color measurements” section, was measured with the system developed in this work. For these set of *CVS* measurements, the Nikon camera and the quadratic plus interactions model were used. In the image processing step, the region of interest of the image was defined by segmentation or was manually selected. Since the color conversion is performed pixel by pixel, a large quantity of information and details were obtained. For example, Fig. 2 depict a beef sample and the surface distribution of the $L^*a^*b^*$ color parameters. As can be seen, the color of the different components (muscle, bone, fat) can be distinguished.

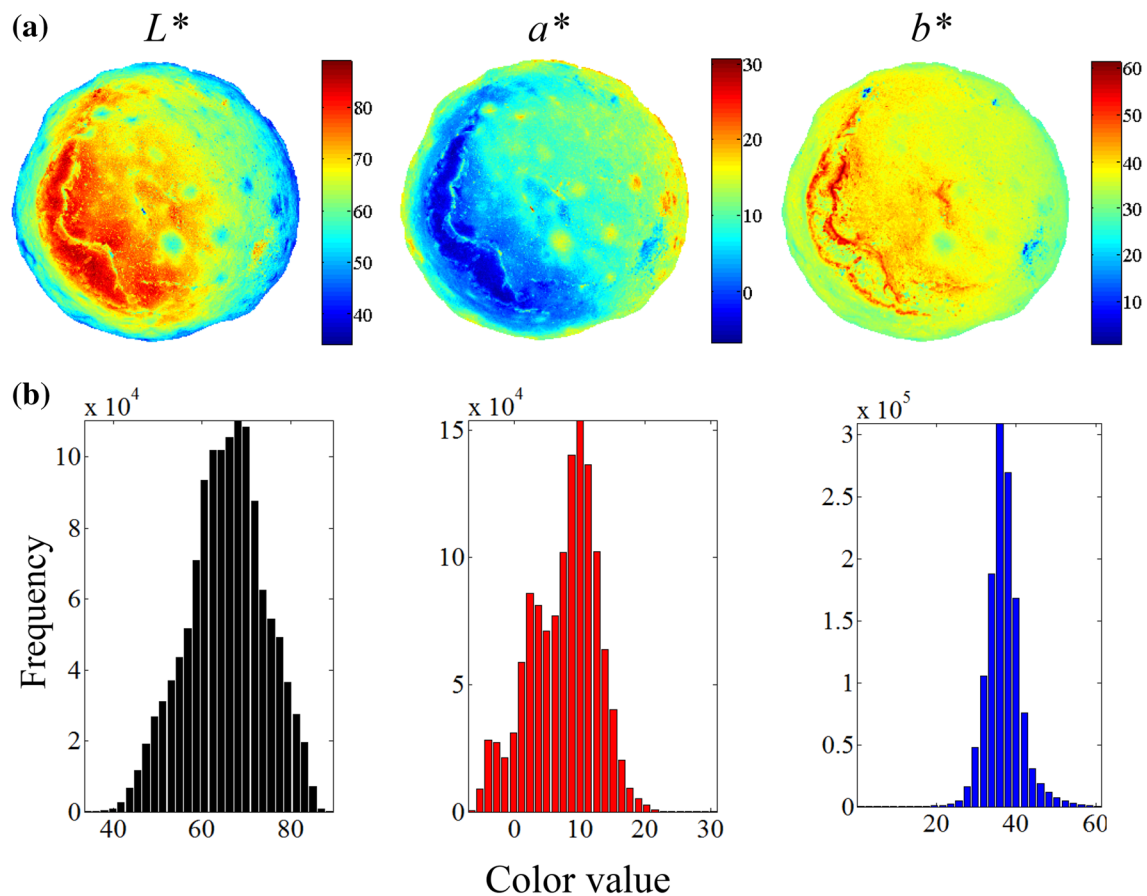


Fig. 6 Color values obtained with the CVS for the sponge cake sample. **a** Surface distributions of $L^*a^*b^*$ values. **b** Histogram of $L^*a^*b^*$ values. (Color figure online)

CVS vs. colorimeter measurements

As indicated in “Color measurements” section, the results provided by the CVS were compared with color values obtained with a traditional colorimeter. As can be seen in Fig. 3 good agreement was obtained for the whole set of food samples tested in this work, being the correlation coefficient equal to 0.971, 0.956 and 0.977, for L^* , a^* and b^* , respectively. The test of hypothesis on the equality of the means was accepted in the 92.5, 87.5 and 80.0% of the cases, for L^* , a^* and b^* , respectively. At first instance, these results indicate that both systems are equivalent to quantify the color parameters, for most samples. However, the average color difference between both methods, considering the 40 samples, was $\Delta L^* = 2.79 \pm 2.42$, $\Delta a^* = 3.02 \pm 2.94$, $\Delta b^* = 2.84 \pm 2.53$, and the average total color difference was $\Delta E = 5.88 \pm 3.32$, with 37 of 40 samples with ΔE greater than 2. These differences are high enough to be noticeable, and then both systems are not equivalent. The largest ΔE between the two systems was obtained for the breast chicken, $\Delta E = 13.47$, and the smallest one was recorded for the white glazed cookie, $\Delta E = 0.67$. In general, the glazed cookies presented the lowest color differences, probably due

to that these samples are the less translucent, then the colorimeter light does not largely penetrate the food’s surface. Others researchers also informed color values measured by both approaches, from these values the total color difference ΔE was calculated in this work. Thus, a total color difference ΔE near 5.3 was obtained for a potato chip [26]; an average ΔE near 29.6 was calculated for different dose irradiated Atlantic salmon fillets [30]; and finally ΔE near 19.6 was obtained for samples of different meats [31].

In general the CVS led to color predictions more similar (visually) to the samples, which agrees with other reported results [30, 31]. To illustrate this fact, Fig. 4 depict the predicted color of different samples, obtained by inverting the measured $L^*a^*b^*$ values back to RGB values using the theoretical conversion model. As can be seen, the color predicted with the CVS is closer to the sample than the color read by the colorimeter. In general, the color obtained by the colorimeter was darker, which can be related to the penetration length of the light into the samples. Girolami et al. [31] provided a suitable explanation of the differences obtained between the two approaches. The solid foods are translucent in some extend, then a fraction of the light passes through the surface, and the remaining is reflected. The light that penetrates the sample is

Table 3 Minimum and maximum $L^*a^*b^*$ values of food samples obtained with the colorimeter and the *CVS* (using the quadratic plus interaction model)

	L^*	a^*	b^*
Minimum color values			
Colorimeter	$L^*=27.0$ $a^*=20.2$ $b^*=8.5$	$L^*=60.7$ $a^*=-19.2$ $b^*=44.2$	$L^*=34.7$ $a^*=40.8$ $b^*=-14.8$
Sample	Nectarine, dark region	Green apple	Purple cabbage
<i>CVS</i>	$L^*=25.1$ $a^*=18.6$ $b^*=9.0$	$L^*=63.9$ $a^*=-23.4$ $b^*=48.8$	$L^*=33.5$ $a^*=36.1$ $b^*=-20.1$
Sample	Nectarine, dark region	Green apple	Purple cabbage
Maximum color values			
Colorimeter	$L^*=84.2$ $a^*=-8.8$ $b^*=22.6$	$L^*=34.7$ $a^*=40.8$ $b^*=-14.8$	$L^*=73.2$ $a^*=4.01$ $b^*=68.8$
Sample	Yellow glazed cookie	Purple cabbage	Lemon
<i>CVS</i>	$L^*=86.3$ $a^*=-6.5$ $b^*=19.8$	$L^*=52.3$ $a^*=40.5$ $b^*=35.1$	$L^*=63.5$ $a^*=35.5$ $b^*=64.9$
Sample	Yellow glazed cookie	Nectarine, light region	Orange

The values of interest of each column are highlighted in bold

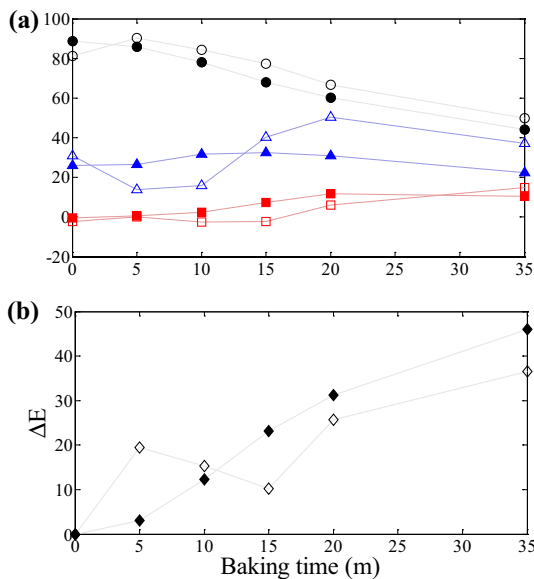


Fig. 7 Browning kinetics of a muffin sample during baking. Filled and open symbols represent colorimeter and *CVS* measurements, respectively. **a** L^* (filled circle, open circle), a^* (filled square, open square) and b^* (filled triangle, open triangle) color values. **b** ΔE values. (Color figure online)

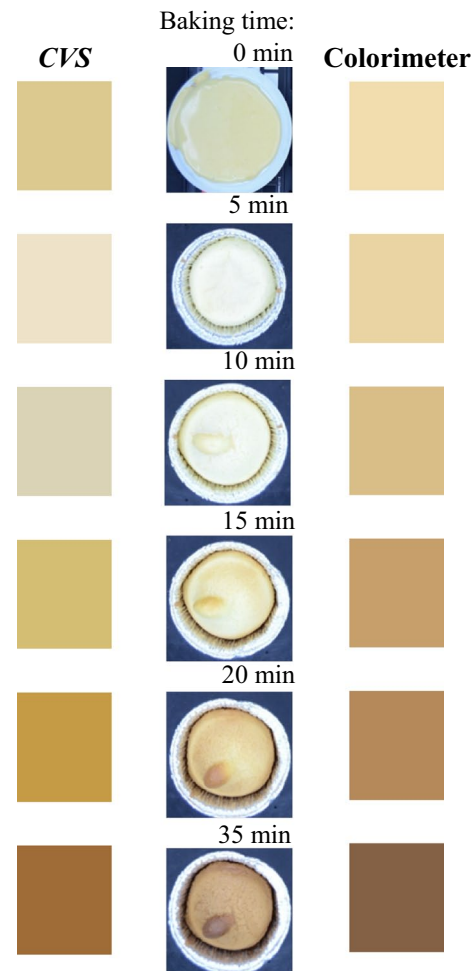


Fig. 8 Muffin color during baking predicted from colorimeter and *CVS* measurements. (Color figure online)

then partially scattered out and diffused in the sample. This phenomenon is affected, among other factors, by the penetration length of the light, which is very different between a colorimeter and a lamp located far of the sample surface. So, the light reflected, which finally affects the measured $L^*a^*b^*$ values, is also different. In beef samples, Girolami et al. [31] found that the light from a colorimeter penetrates about 15–20 mm, and about 5 mm from the *CVS*, similarly Trindrup et al. [25] estimated that light penetrates about 20 mm from a colorimeter, and a few mm from the *CVS*.

An advantage of the *CVS* compared to the colorimeter, is the capability to measure a extend surface, with non uniform color, in a unique image. In this case, several measurements must be done with the colorimeter to obtain a representative color value. Figure 5 presents an image of a sponge cake sample (approx. 255 cm² top surface area), and the color values measured with the colorimeter at 10 selected points. At the same points the color was predicted with the software by selecting small regions of pixels. The average $L^*a^*b^*$ values obtained with the colorimeter were 64.79, 9.35 and 35.48,

respectively, and for the *CVS* were 65.25, 7.70 and 36.70, respectively. Figure 6a show the surface color distribution for the sponge cake, while Fig. 6b shows the corresponding histograms. Besides, the *CVS* allows selecting the whole area as region of interest, being the average L^* , a^* and b^* values equal to 65.59, 7.60 and 36.88, respectively (with standard deviation equal to 8.82, 5.12 and 4.33, for L^* , a^* and b^*).

Table 3 presents the extreme values (minimum and maximum) obtained with the *CVS* as well as with the colorimeter, showing that almost always the results are concordant: the same foods present the minimum $L^*a^*b^*$ values as well as the maximum L^* value, independently of the color measurement technique. In spite of this, ΔE between measurement systems were noticeable.

Sometimes, it is useful to follow the total color difference (measured respect to the initial state) vs. the processing time. Then, ΔE could be similar for both devices. As an example, Fig. 7a shows the color values of a muffin's surface during its baking process. In this type of product, monitoring the browning kinetics helps to define process times [37]. L^* and a^* color values were similar for both devices, larger differences were found for b^* values. Figure 7b shows ΔE values; important differences are observed at the start of baking, but the curves are similar at the end of baking. Figure 8 shows a sequence of images, obtained from both techniques, illustrating the evolution of muffin's color during its baking process. Both image sequences satisfactorily represent the browning, although the color predicted from the colorimeter measurements seems darker, in agreement with the measured L^* values.

Conclusions

In this work, the *CIELAB* color of foods samples of diverse nature was measured using a traditional tristimulus colorimeter and predicted with a computer vision system (*CVS*) and image analysis. The *CVS* allows obtaining the *CIELAB* color parameters from common *RGB* images, through a suitable calibration process. The main image processing was performed by means of software developed *ad-hoc*, in the form of simple and user friendly graphics interfaces, available for its free download.

The color obtained with both devices was highly correlated, and a great number of samples were considered equal based on suitable test of hypothesis. However the total color difference was high enough to be noticeable for most samples, concluding that both systems are not equivalent. On the other hand, the color predicted from *CVS* lead to color predictions that visually better resembles the samples.

Acknowledgments Authors acknowledge Consejo Nacional de Investigaciones Científicas y Técnicas (CONICET, PIP

11220120100180), Agencia Nacional de Promoción Científica y Tecnológica (ANPCyT PICT 2013-1637), and Universidad Nacional de La Plata (UNLP, I183; Subsidios Jóvenes Investigadores 2012) from Argentina for their financial support; Dr. D. F. Olivera and Dr. M. M. Ureta for the muffin and sponge cake samples.

References

1. P.B. Pathare, U.L. Opara, F. Al-Julanda Al-Said, Colour measurement and analysis in fresh and processed foods: a review. *Food Bioprocess Tech.* **6**, 36–60 (2013)
2. D. Wu, D.-W. Sun, Colour measurements by computer vision for food quality control: a review. *Trends Food Sci. Tech.* **29**, 5–20 (2013)
3. Commission Internationale de l'Eclairage CIE DS 014–4.3/E: 2007. Colorimetry—Part 4: CIE 1976 $L^*a^*b^*$ colour space. (CIE Central Bureau, Vienna, 2007)
4. C.-J. Du, D.-W. Sun, Recent developments in the applications of image processing techniques for food quality evaluation. *Trends Food Sci. Tech.* **15**, 230–249 (2004)
5. S. Cubero, N. Aleixos, E. Moltó, J. Gómez-Sanchis, J. Blasco, Advances in machine vision applications for automatic inspection and quality evaluation of fruits and vegetables. *Food Bioprocess Tech.* **4**, 487–504 (2011)
6. L. Fernández, C. Castellero, J.M. Aguilera, An application of image analysis to dehydration of apple discs. *J. Food Eng.* **67**, 185–193 (2005)
7. F. Mendoza, P. Dejmeck, J.M. Aguilera, Calibrated color measurement of agricultural foods using image analysis. *Postharvest Biol. Technol.* **41**, 285–295 (2006)
8. S.P. Kang, A. R. East, F.J. Trujillo, Colour vision system evaluation of bicolour fruit: a case study with 'B74' mango. *Postharvest Biol. Technol.* **49**, 77–85 (2008)
9. E. Purlis, V.O. Salvadori, Bread browning kinetics during baking. *J. Food Eng.* **80**, 1107–1115 (2007)
10. R.E. Larraín, D.M. Schaefer, J.D. Reed, Use of digital images to estimate CIE color coordinates of beef. *Food Res. Int.* **41**, 380–385 (2008)
11. M. Mohebbi, M.-R. Akbarzadeh-T, F. Shahidi, M. Moussavi, H.-B. Ghodduzi, Computer vision systems (CVS) for moisture content estimation in dehydrated shrimp. *Comput. Electron. Agric.* **69**, 128–134 (2009)
12. I. Arzate-Vázquez, J.J. Chanona-Pérez, M. de Jesús Perea-Flores, G. Calderón-Domínguez, M.A. Moreno-Armendáriz, H. Calvo, S. Godoy-Calderón, R. Quevedo, G. Gutiérrez-López, Image processing applied to classification of avocado variety Hass (*Persea americana* Mill.) during the ripening process. *Food Bioprocess Tech.* **4**, 1307–1313 (2011)
13. G. Romano, D. Argyropoulos, M. Nagle, M.T. Khan, J. Müller, Combination of digital images and laser light to predict moisture content and color of bell pepper simultaneously during drying. *J. Food Eng.* **109**, 438–448 (2012)
14. M. Dowlati, S.S. Mohtasebi, M. Omid, S.H. Razavi, M. Jamzad, M. de la Guardia, Freshness assessment of gilthead sea bream (*Sparus aurata*) by machine vision based on gill and eye color changes. *J. Food Eng.* **119**, 277–287 (2013)
15. S. Hosseinpour, S. Rafiee, S.S. Mohtasebi, M. Aghbashlo, Application of computer vision technique for on-line monitoring of shrimp color changes during drying. *J. Food Eng.* **115**, 99–114 (2013)
16. E. Saldaña, R. Siche, W. Castro, R. Huamán, R. Quevedo, Measurement parameter of color on yacon (*Smilax sonchifolius*) slices using a computer vision system. *LWT Food Sci. Technol.* **59**, 1220–1226 (2014)

17. N. Vélez-Rivera, J. Blasco, J. Chanona-Pérez, G. Calderón-Domínguez, M. de Jesús Perea-Flores, I. Arzate-Vázquez, S. Cubero, R. Farrera-Rebollo, Computer vision system applied to classification of “manila” mangoes during ripening process. *Food Bioprocess Tech.* **7**, 1183–1194 (2014)
18. A. Iqbal, N.A. Valous, F. Mendoza, D.-W. Sun, P. Allen, Classification of pre-sliced pork and Turkey ham qualities based on image colour and textural features and their relationships with consumer responses. *Meat Sci.* **84**, 455–465 (2010)
19. R.A. Quevedo, J.M. Aguilera, F. Pedreschi, Color of salmon fillets by computer vision and sensory panel. *Food Bioprocess Tech.* **3**, 637–643 (2010)
20. D. Mery, BALU: A toolbox Matlab for computer vision, pattern recognition and image processing (2011). <http://dmery.ing.puc.cl/index.php/balu>. Accessed 10 Sept 2015
21. P. Jackman, D.-W. Sun, G. ElMasry, Robust colour calibration of an imaging system using a colour space transform and advanced regression modeling. *Meat Sci.* **91**, 402–407 (2012)
22. L. Gómez-Robledo, N. López-Ruiz, M. Melgosa, A.J. Palma, L.F. Capitán-Vallvey, M. Sánchez-Marañón, Using the mobile phone as Munsell soil-colour sensor: an experiment under controlled illumination conditions. *Comput. Electron. Agr.* **99**, 200–208 (2013)
23. D. Mery, F. Pedreschi, A. Soto, Automated design of a computer vision system for visual food quality evaluation. *Food Bioprocess Tech.* **8**, 2093–2108 (2013)
24. H. Manninen, M. Paakki, A. Hopia, R. Franzén, Measuring the green color of vegetables from digital images using image analysis. *LWT Food Sci. Technol.* **63**, 1184–1190 (2015)
25. C. Trinderup, Y.H.B. Kim, Fresh meat color evaluation using a structured light imaging system. *Food Res. Int.* **71**, 100–107 (2015)
26. K. León, D. Merry, F. Pedreschi, J. León, Color measurement in L*a*b* units from RGB digital images. *Food Res. Int.* **39**, 1084–1091 (2006)
27. N.A. Valous, F. Mendoza, D.-W. Sun, P. Allen, Colour calibration of a laboratory computer vision system for quality evaluation of pre-sliced hams. *Meat Sci.* **81**, 132–141 (2009)
28. W. Dana, W. Ivo, Computer image analysis of seed shape and seed color for flax cultivar description. *Comput. Electron. Agr.* **61**, 126–135 (2008)
29. F.J. Rodríguez-Pulido, L. Gómez-Robledo, M. Melgosa, B. Gordillo, M.L. González-Miret, F.J. Heredia, Ripeness estimation of grape berries and seeds by image analysis. *Comput. Electron. Agr.* **82**, 128–133 (2012)
30. Y. Yagiz, M.O. Balaban, H.G. Kristinsson, B.A. Welt, M.R. Marshall, Comparison of Minolta colorimeter and machine vision system in measuring colour of irradiated Atlantic salmon. *J. Sci. Food Agr.* **89**, 728–730 (2009)
31. A. Girolami, F. Napolitano, D. Faraone, A. Braghieri, Measurement of meat color using a computer vision system. *Meat Sci.* **93**, 111–118 (2013)
32. R.C. Gonzalez, R.E. Woods, in *Digital Image Processing* (2nd edn). (Prentice Hall, New Jersey, 2002)
33. IEC 61966-2-1, Colour Measurement and Management in Multimedia Systems and Equipment—Part 2-1: default RGB Colour Space-sRGB. 1° Ed. (1999)
34. B. Pace, M. Cefola, F. Renna, M. Renna, F. Serio, G. Attolico, Multiple regression models and Computer Vision Systems to predict antioxidant activity and total phenols in pigmented carrots. *J. Food Eng.* **117**, 74–81 (2013)
35. Pascale, D. (2006). RGB Coordinates of the Macbeth ColorChecker. http://www.babelcolor.com/index_htm_files/RGBCoordinatesoftheMacbethColorChecker.pdf. Accessed 12 Feb 2016
36. W.W. Hines, D.C. Montgomery, *Probability and Statistics in Engineering and Management Sciences* (3rd edn). (Wiley, Inc, New Jersey, 1990)
37. M.M. Ureta, D.F. Olivera, V.O. Salvadori, Baking of muffins: kinetics of crust color development and optimal baking time. *Food Bioprocess Tech.* **7**, 3208–3216 (2014)